NOTICE CONCERNING COPYRIGHT RESTRICTIONS

3D Subsurface Modeling of Gümüşköy Geothermal Area, Aydın, Turkey

Sertaç Akar[1], Ozan Atalay[1], Ö. Çağlan Kuyumcu[1], Umut Z. D. Solaroğlu[1], Burcu Çolpan[1], Sadun Arzuman[2]

[1]BM Engineering and Construction Inc., Ankara, Turkey
[2]Schlumberger Information Solutions, Ankara, Turkey

Keywords

3D geology model, structural framework, magnetotelluric, subsurface temperature, geothermal system, Gümüşköy, Turkey

ABSTRACT

Most of the geothermal systems in Turkey are in Western Anatolia. Geothermal energy power plant (GEPP) capacity in this area is 87 MW, with a further 200 MW of capacity under construction. The Gümüşköy geothermal project is at the westernmost boundary of Büyük Menderes graben (BMG) with an initial capacity of 25 MW. BM Engineering and Construction Inc. started exploration studies for Gümüşköy in 2005. Studies completed so far include: geology, geochemistry, geophysics, and numerous shallow and deep wells. The geothermal system of Gümüşköy can be defined as a hot-water-dominated convective hydrothermal resource with deep circulation of water along fractures in the BMG.

Previous studies were carried out with the limited scope of a 2D approach, but they did not provide a better understanding of the study area. A 3D earth model of the Gümüşköy geothermal area was generated to visualize and analyze the subsurface geology and geothermal system using existing information. For this purpose, petrel software was used to prepare lithology, structural geology, geophysics, and thermal models in 3D within the study area.

The 3D modeling methodology comprised four stages: data input, structural modeling, property modeling, and uncertainty analysis. In structural modeling, a 3D fault model was generated and a 3D grid system was created. Three-dimensional subsurface geology, magnetotelluric (MT) resistivity, and temperature models were generated using both deterministic and stochastic approaches. Additionally, uncertainty analysis was conducted by applying probabilistic methods.

All relevant data was combined to build a fit-for-purpose model, which has been validated by a new well drilled in the area. The 3D subsurface model helped in visualizing and understanding the structural framework, geology, and interactions with the geothermal system. This model will be used as the basis of a 3D numerical dynamic flow model of the existing reservoir.

1. Introduction

Western Anatolia is one of the most active tectonic and seismic areas in the world, with an accepted strong geothermal potential. Geothermal systems of Western Anatolia appear in areas of complex tectonics with strike-slip and normal faults, and feature complex geochemistry.

Previous studies show that the Menderes Massive has a high surface heat flow (100–300 mW/m²) and Curie depth points from 6 km to 12.4 km. (İlkışık, 1995; Aydın et al., 2005; Dolmaz, 2005; Akın et al., 2007). Active known geothermal sites of Büyük Menderes graben (BMG) from east to west along the northern boundary fault are: Kızıldere (242ºC), Pamukören (188ºC), Nazilli-Gedik, Sultanhisar (146ºC), Salavatlı (171ºC), Yılmazköy (142ºC), Germencik (232ºC) and Bozköy-Çamur (142ºC) (MTA, 2005).
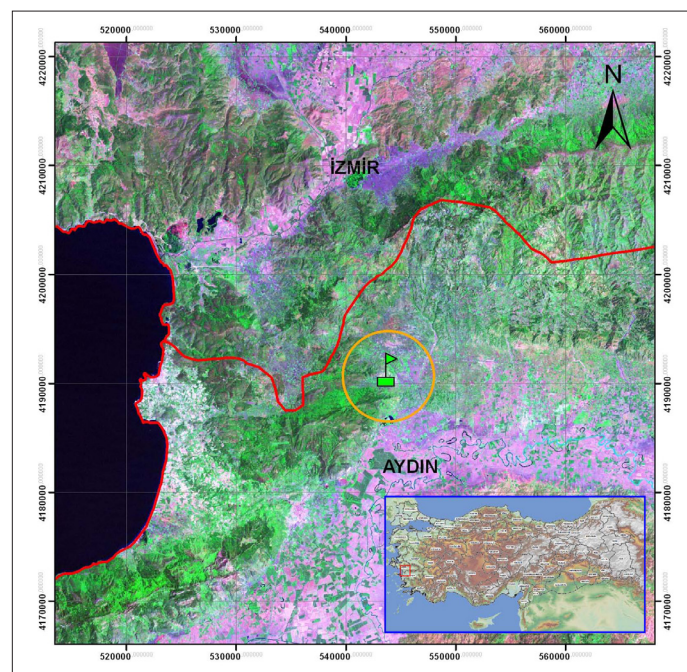

Figure 1. Location map of the study area.

The study area is located on the western part of the BMG, near Aydın, Turkey (Figure 1). The area is close to the Germencik geothermal site, which has reservoir temperatures reaching up to 232ºC. The Gümüşköy geothermal area was previously studied and ultimately discarded in 2004 by the Mineral Research and Exploration General Directorate (MTA), owing to very limited surface indications and a failed shallow exploration well.

The exploration studies carried out in Gümüşköy by BM Engineering started in 2005, with geological, geochemical, and geophysical surveys. Three gradient wells were drilled in the area using the information received from surface indications, supported by 3D magnetotelluric (MT) and time domain electromagnetic (TDEM) studies. The first exploration well was completed in 2009 with a depth of 2,100 m, yielding a flow rate of 216 tons/hour. It also had a maximum reservoir temperature of 181ºC, which was the strongest confirmation of the presence of geothermal resources in the Gümüşköy area. Two further exploration wells were drilled to 2,057 m and 2,334 m, having reservoir temperatures of 165ºC and 130ºC and flow rates of 152 tons/hour and 126 tons/hour respectively.

2. Regional Geology

The Menderes Massive is a major metamorphic complex in Western Turkey, bearing imprints of Precambrian and Eocene metamorphic and deformational events (Şengör et al., 1984; Bozkurt and Oberhänsli, 2001). The Menderes Massive has a complex nappe-pile structure developed during the closing of Neotethys, consisting of different tectonic slices including metamorphic and metaophilitic rocks (Ring et al., 1999, 2003). Pan-African intense deformation and eclogitic metamorphism affected only the core of the Massive, and deformation by regional amphibolites facies metamorphism with local anatexis followed (Rimmelé et al., 2004; Şengör et al., 1984; Candan et al., 2001).

Southwestern Turkey, including the Menderes Massive, has been affected by an extensional tectonic regime since the Oligocene Epoch (Bozkurt and Satir 2000; Bozkurt and Oberhänsli, 2001; Gessner et al., 2001). The neotectonic domain of Southwestern Turkey is characterized by a tensional tectonic regime and distributed stress system, characterized by multidirectional extension. The main structures characterizing and shaping this neotectonic domain are the graben-horst systems and their margin-boundary normal faults. The E-W trending Menderes graben is divided into several sub-grabens and sub-horsts along its western tip around Ortaklar, Gümüşköy, Argavlı, and Kirazlı (Koçyiğit, 2009).

The stratigraphy of the study area can be subdivided into three different groups. The oldest group, the Pan-African basement, is only found in the south of the BMG and is defined by augen gneisses. The second group, the Cycladic metamorphic complex, mainly consists of metasedimentary rocks ranging in age from Paleozoic to Tertiary (Bozkurt and Oberhänsli, 2001; Okay, 2001). The third group consists of Neogene and younger sedimentary rocks that unconformably overlie older metamorphic units.

The Menderes Massive is separated into four different nappes. From base to top, these are: a) Dipburun Nappe, b) Efes Nappe, c) Şirince Nappe, and d) Bodrum Nappe (Çakmakoğlu, 2007). The Dipburun Nappe does not crop out in the study area. The Efes Nappe rests tectonically on the Dipburun Nappe in the Dilek Peninsula and comprises presumed Late Paleozoic-Early Triassic schist, gneiss and marble alternations (the Meryemana formation) at the base, and presumed Triassic-Late Cretaceous marbles (The Ayrıcadağ formation) at the top (Figures 2a, 2b). Şirince Nappe comprises a chaotic metamorphic unit (Şirince Metaflysch). The Bodrum Nappe consists of Early-Middle Triassic metaclastics and overlying Middle Triassic-Cenonian carbonates (Çakmakoğlu, 2007).
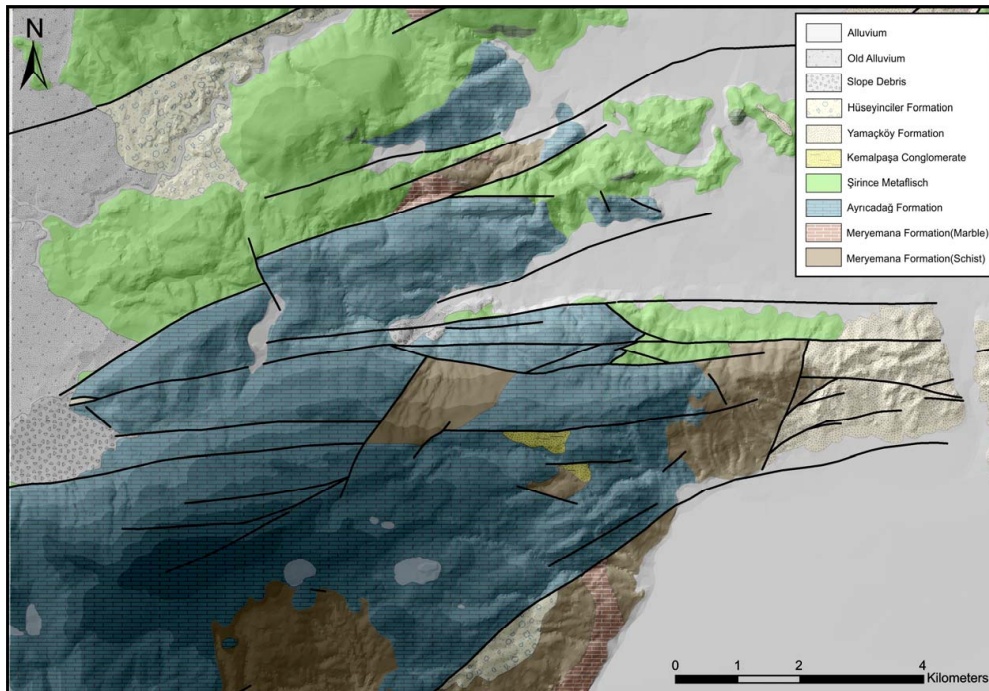

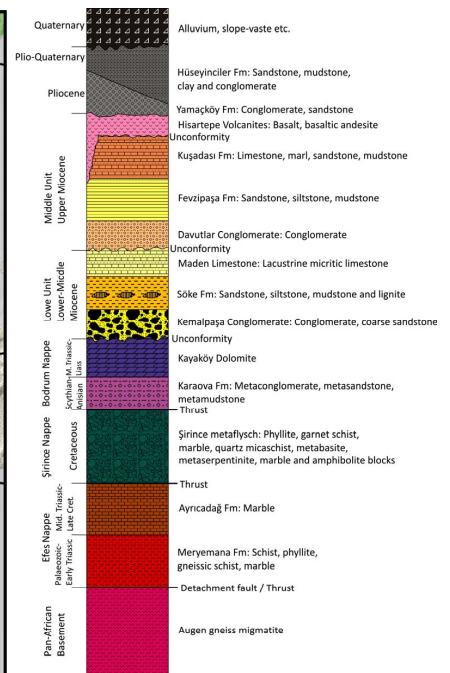**Figure 2a.** Gelological map of the study area (Tüysüz and Genç, 2010).

Figure 2b. Generalized stratigraphic column (Tüysüz and Genç, 2010).

3. Geothermal System

Completed studies have so far revealed that horst-graben systems and their margin-boundary active normal faults in Söke graben and the Gümüşköy sub-graben create pathways for underground circulation of hot fluids. Their upwelling to shallower depths gives rise to indications such as hot water springs. The main sources of heat in the study area are thinning of the Earth's crust and relatively young felsic igneous rock intrusions. The He³/He⁴ and R/Ra content of hot waters in this region reveals that there is crustal thinning reaching up to 25 km beneath the Aegean Sea and the adjacent terrestrial areas in the period of last 45 Ma. Accordingly, the asthenosphere welled up to shallow depths (Pfister et al. 1997). Hisartepe volcanics are exposed in the form of necks and domes in the north and northwest of Söke County in the study area, and this is viewed as another source of heat.

Suitable reservoir rocks for the geothermal system are the Upper Paleozoic to Mesozoic highly fractured marbles and intensely sheared, crushed, fractured and brecciated schists in the study area. These thick and highly porous reservoir rocks are overlain with an angular unconformity. This, in turn, is overlain by a 0.5 km thick and strongly lithified cover sequence composed of fluvio-lacustrine sediments, including conglomerate, sandstone, siltstone, shale, marl, and lacustrine limestone alternation. This sequence prevents the escape of hot underground fluids from the reservoir (Koçyiğit, 2009).

Hot and mineralized water from most discharges is of neutral weakly alkaline Na-Cl (-HCO$_3$) type. Tritium isotope and chloride data indicates that the hot waters discharging from Gümüşköy district are caused by a mixture of meteoric and marine origin. The marine content in the mixture is fairly low. According to alkali and silica geothermometer calculations, the reservoir temperature ranges from 130ºC to 190ºC. This variation means there is no full equilibrium in the field for fluid chemistry. CaCO$_3$ scaling seems to be common owing to its ionic content and pH values, whereas SiO$_2$ scaling is not a great risk (Yıldırım, 2009). In general, the Gümüşköy geothermal area can be identified as a hot-water-dominated convective hydrothermal resource. This system results from deep circulation of water along fractures present in the BMG.

4. 3D Subsurface Model

Previous studies for geological modeling were based on 2D interpretations of cross sections, maps, well logs, and geophysical surveys. A 3D modeling approach appeared to be crucial to make further progress in the study. Modeling in 3D provides the ability to interpolate the geometry of structure and is an effective way of understanding geological features.

4.1 Available Data

The data sources used in the study varied and were as follows:

- **Maps and cross sections:** *Surface and structural geology, digital topography, lineaments (from remote sensing), and geological cross sections*
- **Well data:** *Lithology logs, gamma ray (GR), resistivity, sonic, formation micro-imager, pressure, temperature,* *spinner, and drilling parameter logs [such as rate of penetration (ROP), weight on bit (WOB), and mud-in/out].*
- **Geophysical data:** *3D MT with TDEM, gravity, and seismicity.*
- **Geochemistry data:** *Elemental analysis (*major anions and cations*), isotope analyses [¹⁸O/¹⁶O and Hydrogen/Deuterium (H/D)].*

Surface geology and neotectonic maps were prepared by BM Engineering consultants, and available literature was also used. Digital elevation data were obtained from topography maps, and a digital elevation model (DEM) was derived from ASTER satellite images. Lineament data were created using stereographic images from ASTER.

Lithology information was extracted from cuttings and cores of wells, and composite logs were generalized into main formations and facies. Geological cross sections in the study area were used to define subsurface geology. There are 22 wells of various depths in the study area: 3 exploration wells with depths of approximately 2,000 m, 12 temperature gradient wells with 250-m to 1,000-m depths, 6 cold-water wells, and 1 reinjection well. Conventional logs (such as GR, self potential (SP), resistivity, and microimager logs) are available for two exploration wells. Temperature and pressure logs are also available in 13 wells, and spinner logs are present in 3 wells.

MT data was repeatedly acquired over the study area from 2007 to 2009. During three acquisition stages, MT data was collected from 393 stations with a 1×1 km surface interval. Data collected in this study was analyzed using 0.5×0.5 km constant horizontal and 25 m to 90 m decreasing vertical resolution (Geosystem, 2008). Seismicity data (magnitudes > 3 in Richter scale) was obtained from Boğaziçi University Kandilli Observatory and Earthquake Research Institute for the years 1900 to 2008 over the whole region in 100 km radial vicinity (KOERI, 2010). Regional gravity data collected by Turkish Petroleum Company (TPAO) and MTA were also incorporated to the study.

4.2 Methodology

The 3D modeling methodology utilized in this study includes four stages: data input, structural modeling, property modeling, and uncertainty analysis (Figure 3). Dimensions of the 3D subsurface model were 14 km × 9 km horizontal and 2.5 km vertical, with a volume of 315 km³. The data input stage includes both conventional and GIS format data. Structural modeling defines the skeleton of the 3D model, including faults, horizons, and zones. In the property modeling stage, 3D subsurface models [such as lithology, magnetotelluric (MT) resistivity, and temperature] were generated. The lithology model was built using both deterministic and stochastic approaches. The deterministic approach yielded more realistic results because there were limited wells in the study area. The temperature model was built with different algorithms such as minimum curvature and Gaussian random function simulation (GRFS) with collocated cokriging. Overall, GRFS with collocated cokriging was found to be the optimum solution. Additionally, an uncertainty analysis was conducted on the selected model with probabilistic calculations.

In the first stage of the project, well information [including well deviations, well logs, GR, resistivity, sonic, microimager logs,
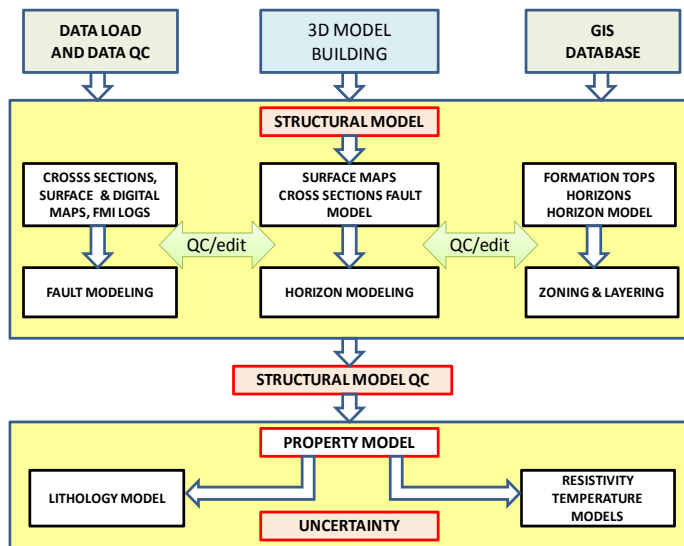
Figure 3. Flowchart of methodology.

pressure/temperature (PT) and pressure-temperature-Spinner PTS logs, and drilling parameters such as ROP, WOB, and circulation temperatures] was incorporated into the study. Anomalies were detected by correlating this information with the lithology logs. GR logs revealed that values lower than 60 API were related to marble, and values higher than 160 API corresponded to gneiss and schists. Spinner logs were converted to flow-rate logs using caliper log information, and peak points of the flow-rate logs were selected to define possible inflow zones. Temperature logs and drilling parameters were also investigated while defining these zones. Possible inflow zones were correlated with faults and foliation planes derived from microimager logs, and a relationship was established. The next step was to import vectoral GIS data (such as surface faults, lineaments, geochemical sample points, and seismicity points) into the model.

MT data were inverted to the depth domain by computation of a forward response, and the model was modified based on the differences between the observed and computed data (Geosystem, 2008). Two-dimensional vertical and horizontal derivatives of gravity data were used to cross-check the quality of the model.

In the second stage of the project, faults derived from microimager logs were extended to the ground surface, and their ground traces were correlated with surface structural maps and ASTER lineaments to define the 3D fault geometry. Thus, a 3D fault model was generated.

Formation tops were imported to the simulation software database using fence diagrams generated from cross sections, and data quality was checked. Lithology information, together with information relating to alteration minerals gathered from the composite logs, was incorporated into the project. Minor editing was also performed to maintain consistency. Thus, formation horizon surfaces were generated.

Formation boundaries of Quaternary alluvium—Hüseyinciler Fm. (Plio-Quaternary Units), Yamaçköy Fm. (Pliocene Units), and Meryemana Fm. (Paleozoic Metamorphic Units), which were defined by MTA—were merged with the cross sections at a basin scale (Figure 4).
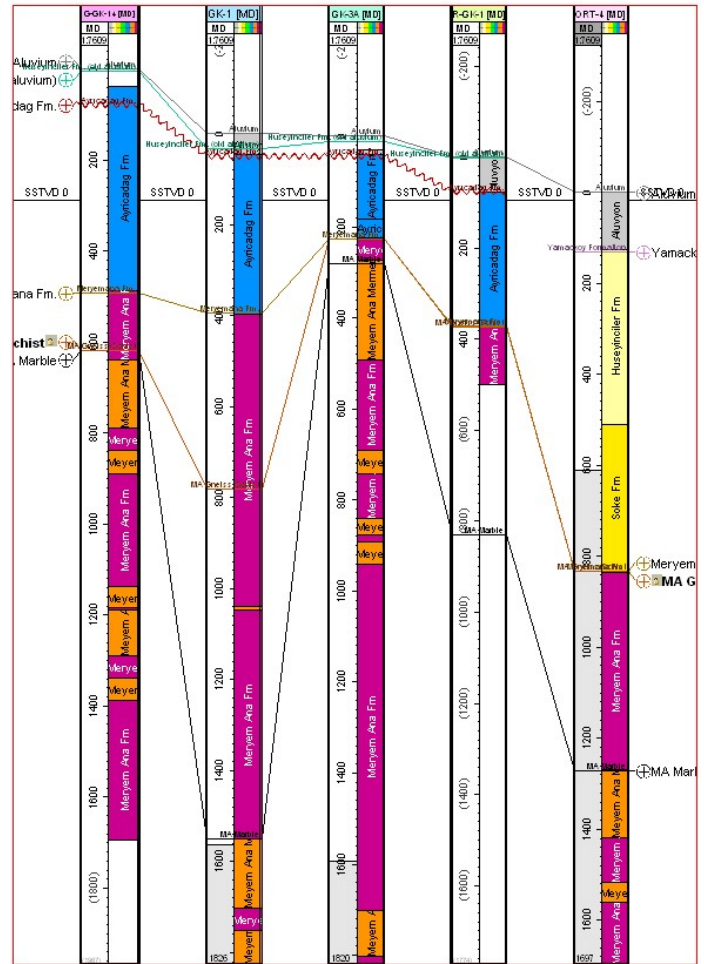

Figure 4. Lithological correlation between wells.

A 3D grid, which forms the skeleton of the model, was then generated based on the fault model. Horizons and zones were defined using formation tops, and layering was performed for each zone.

In the third stage of the project, suitable well logs were upscaled, the MT model was resampled, and appropriate algorithms were utilized to generate lithology and temperature models.

Finally, uncertainty assessment was conducted to select the most likely case for the generated model using a probability distribution generated after 200 iterations.

4.3 Structural Model

As in other subsurface exploration studies, positioning of the faults in the subsurface in 3D is very important in geothermal exploration. The 3D fault framework was initially built for the study area (Figure 5). Faults were derived from various sources, including surface structure (outcrop) maps, lineament information from GIS database, well cross sections, and microimager logs. Most of the fault surfaces were generated by initially extrapolating surface fault lines to their subsurface position using corresponding dip and azimuth information, followed by calibration to match other subsurface data. Information obtained from microimager logs from two wells was also used to correct geometry of some major faults. Quality control of the fault surfaces was performed with
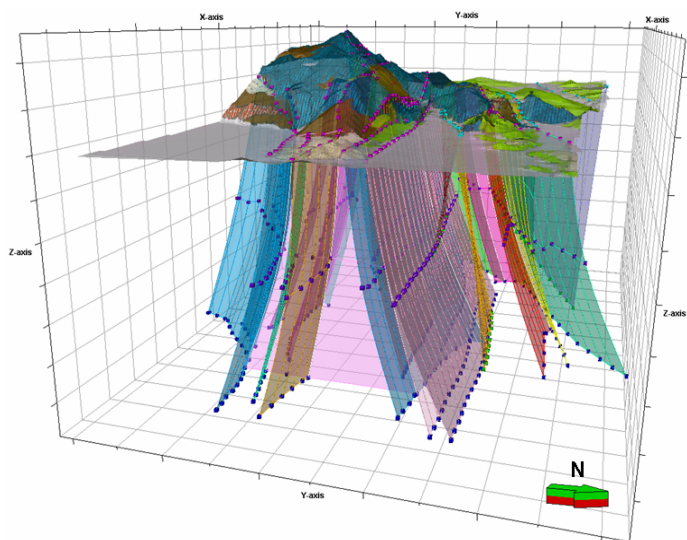
Figure 5. 3D fault model and grid mesh for model skeleton.

Figure 7. 3D subsurface model of the study area.

cross sections derived from geological maps. After completion of the fault model, a 3D grid skeleton with a lateral resolution of 100 m x 100 m was prepared.

Creation of the fault skeleton was followed by inserting the main horizons into the 3D subsurface grid. This process required regridding and repositioning of surfaces near faults to fit results to the model skeleton and allow better representation of displacements across each fault. As the number of data points was insufficient to define lithological boundaries from formation tops, which were the only sources of this data, cross sections were used to digitize horizons within the study area. For this purpose, a fence diagram was created from 10 cross sections (Figure 6). In total, eight horizons were defined, including surface topography and bottom surfaces (Figure 7).

Zoning and layering processes define the fine-scale stratigraphy intervals between main horizons. Since there was insufficient formation top information available in the study area, layering was performed by dividing the main zones into 10 m to 50 m intervals.
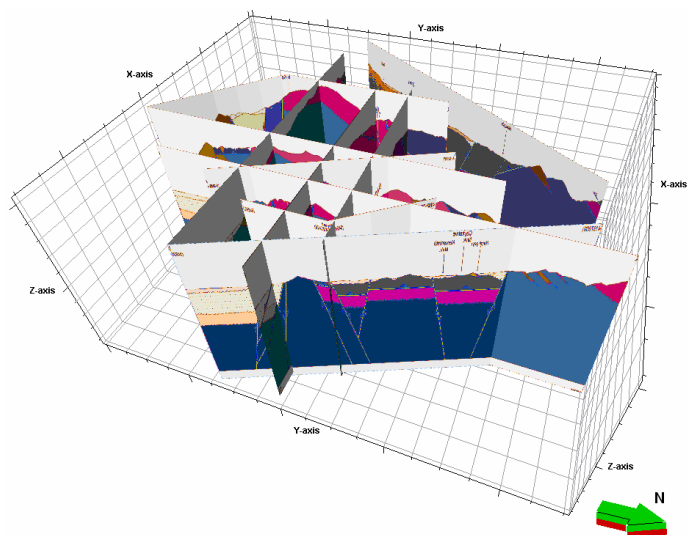
During the layering process, the depositional setting of the sedimentary units was considered. Quality control of the 3D structural grid was performed by checking cells exhibiting irregular shapes. Cross sections were also used for inspection of the whole model to check for possible artifacts.

4.4 Lithology and Property Models

An accurate 3D representation of geological and geothermal variables like temperature, pressure, resistivity, porosity, and permeability is very important to understand a geothermal field. In this study, lithology, resistivity, and temperature properties were modeled.

The model can be generated by either deterministic or stochastic algorithms. The deterministic case simply assigns defined values to proper 3D cells determined by the user. The stochastic case is algorithm-dependent and requires some preprocessing of the data. Preprocessing involves upscaling of well logs or resampling of existing 3D models. The upscaling process involves assigning values to the 3D cells corresponding to well trajectories within the model, using different averaging methods.

First, the lithology of the study area was populated into the 3D subsurface skeleton. Deterministic and stochastic methods
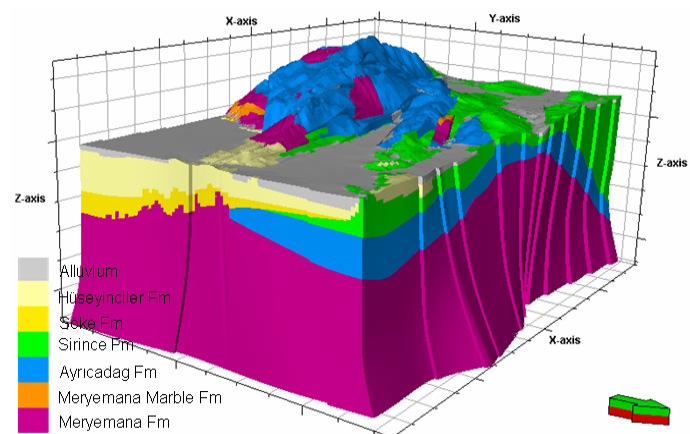

Figure 6. Fence diagram built from cross sections.

Figure 8. Deterministic lithology model.

were used to distribute lithologies inside the 3D model. In the first model, formation boundaries were created from cross sections, and every zone was then populated by assigning corresponding formation values to each cell in the 3D grid (Figure 8). In the second model, lithology logs from eight wells were populated using the indicator simulation (IS) algorithm. A stochastic modeling algorithm, IS uses upscaled lithological logs along with an underlying variogram model.

The main differences between these two models were the type of input data. The first model did not use any well information because it constantly distributed the values defined by the modeler and produced only one output model based on user input. The second method used upscaled logs for formations and the IS stochastic algorithm yielded a heterogeneous representation of the modeled area by producing equally probable multiple realizations.
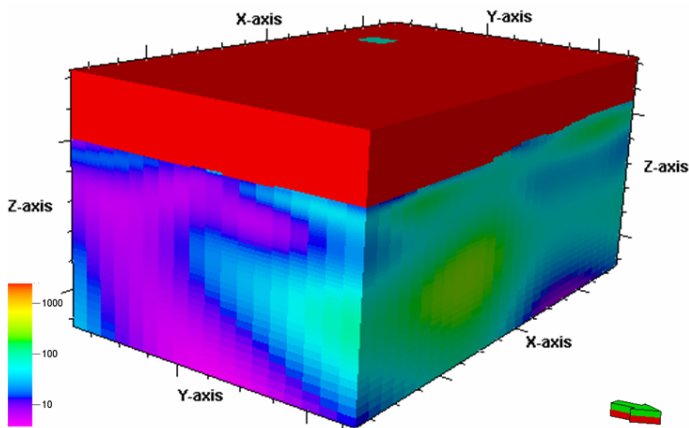

Figure 9a. 3D MT resistivity model (Ωm) in depth domain.

Second, the 3D MT resistivity model was resampled into a 3D subsurface model. Since the cell geometry of the MT model was different than that of the 3D subsurface model, a volume-weighted averaging algorithm was used for resampling (Figures 9a and 9b). In this algorithm, all source cells in 3D MT grid were initially sampled to the overlapping target cell in the model, and the values of source cells corresponding to the target cells were averaged and weighted proportional to the volume (Petrel Online Help, 2010).
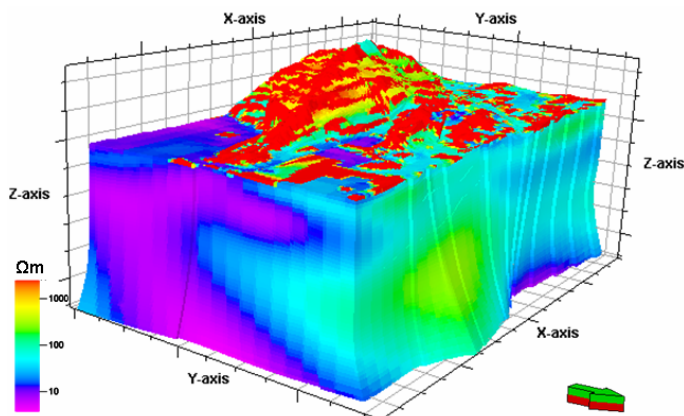

Figure 9b. MT resistivity model (Ωm) resampled into 3D subsurface model.

Temperature modeling was accomplished using static formation temperatures from PT logs. Eight wells with various depths were used and upscaled into a 3D grid. Several algorithms were tested to obtain a more realistic scenario. Initially, the moving average (MA) algorithm was used to distribute the temperature values across the model. This algorithm provided almost constant temperature values within the main stratigraphic intervals, which did not represent the actual subsurface conditions. Therefore, the MA algorithm was utilized using MT resistivity model as a trend (Figure 10).
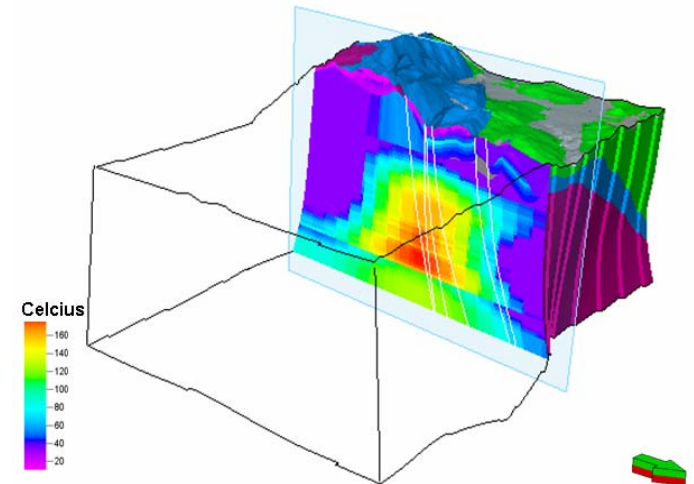
Figure 10. Representation of 3D temperature model generated using moving average algorithm with MT trend.

The GRFS algorithm was also applied for temperature modeling. GRFS is a stochastic simulation algorithm that accounts for spatial variability within the subsurface by keeping covariance unchanged, and adding random and independent component to variance (Petrel*, 2010).

Two different GRFS models were built. The first model used only upscaled temperature logs as an input with an underlying variogram model, and the result was mostly a random distribution of

Figure 11. Representation of 3D temperature model generated using GRFS with collocated MT cokriging.

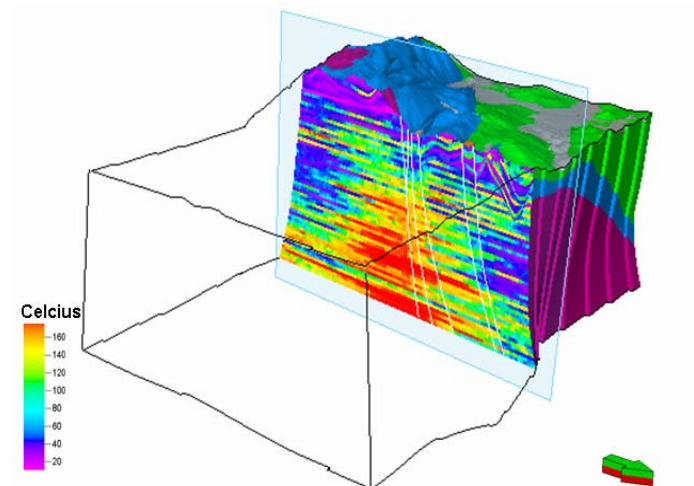temperature values because of the sparse input data. In the second model, MT data was used with collocated cokriging methodology (Figure 11) (Petrel Online Help, 2010).

4.5 Uncertainty Assessment

One of the key factors affecting the 3D model building studies is the uncertainty incorporated into the results. These uncertainties mostly result from input data quality levels and the heterogeneity of the subsurface.

There is no way to control uncertainty in deterministic approaches, but for the stochastic algorithms, uncertainty can be calculated probabilistically. In this study, uncertainty analysis was performed only for temperature models. Structural uncertainty was not included because deterministic methods were deployed to 3D subsurface geology.

In general, the 3D model uncertainties can be assessed as follows:

- Uncertain parameter selection: quantification and ranking of importance.

- Integration of selected parameters: knowing which parameters affect each other.

- Construction of multiple realizations: iterative creation of models using uncertain parameters.

- Decision making: selection of the most probable outcomes.

The uncertainty distribution for the temperature model was prepared with the understanding that producing many realizations using the same input data is likely to generate equally probable results. These realizations were created by defining a starting point (seed number) within the input data matrix (Petrel Online Help, 2010). Two hundred simulations were run for the temperature model, and the most probable outcome was chosen.

5. Discussions and Conclusions

Three major properties were modeled in this study: lithology, resistivity, and temperature. The structural model was built using surface geology maps and lineaments from remote sensing data. The most challenging part of building the structural model was the construction of the fault framework. Faults recognized at the surface were extended to the subsurface using their dip information; among them, only two were carried into the model with microimager log data control. Therefore, quality of the fault positioning was limited to surface geology information. Availability of seismic information in the future may improve the results, despite the imaging problems caused by metamorphic units in the study area.

Lithology model inputs were limited to hand-drawn cross sections. Therefore, a deterministic approach was employed by utilizing the available data to construct a 3D subsurface representation of the main lithological units in the study. The limited number of wells is the only source for the quality control for the lithological boundaries; uncertainty of the layer boundaries is expected to increase away from the well locations. The level of structural uncertainty can be assessed with results from the new wells to be drilled in the area.

A stochastic approach was also applied to build a lithology model, but since the output was composed of randomly distributed 3D cell values without a logical sequence, it was omitted.

A resistivity model was created by resampling the existing MT model. The results of the model showed that resistivity anomalies mostly coincide with a E-W trending fault system. It has also been observed that there is structural control for the conductive zones revealed by MT applications in the deeper parts of the study volume.

A temperature model was built based on static formation temperatures from existing wells. A GRFS stochastic algorithm was used with the MT resistivity model as a secondary variable for collocated cokriging methodology. GRFS produced many equally probable realizations for the temperature model, and the best representative output, P50, was selected based on probability distribution obtained from uncertainty analysis.

After combining all the information received from the 3D models, a conceptual model of the geothermal system of the area was outlined. The results of the study verified that there are two different geothermal systems in the area. These are at the western and southeastern extremes of the model, with maximum observed temperatures of 181ºC and 130ºC respectively. The western reservoir consists of three different reservoir levels: one shallow system, which is basically an up-flow zone, and two deep systems (one with a depth of around 1,000 m to 1,400 m, another with depths greater than 1,900 m). The southeastern geothermal system has only one reservoir level of around 1,400 m. Finally, the findings from a new well drilled on the western reservoir zone were consistent with the predictions of the model.

Although the temperature model is consistent within itself, there were slight ambiguities because MT was the only reference parameter and there were few deep wells. This result can be improved using information received from the new wells drilled in the area. However, the fault and lithology models were very successful in terms of representing subsurface geometry. The quality of these models can be improved by applying additional geophysical surveys such as seismic surveying. Two of the most important parameters in geothermal systems, which were not modeled in the study, are porosity and permeability. As a future study, modeling of 3D permeability distribution by applying Multi Criteria Decision Analysis (MCDA) is being considered.

References

Akın, U., M. Duru, S.S. Kutlu, and E.U. Ulugergerli, 2007, "Heat flow map of Turkey (from magnetic data)," 17th Geophyscical Congress, MTA, Ankara.

Akman, A.Ü., Ö.Ç. Kuyumcu, S. Önç and U.Z. Destegül, 2010, "The Tectonic and Magneto-Telluric Survey Effects on the Geothermal Explorations Around the Menderes Massive in the Western Anatolia, Turkey," GRC Transactions, Vol. 34., pp: 739–745.

Aydın, I., H.I. Karat, and A. Koçak, 2005, Curie-Point Depth Map of Turkey, Geophys. J. Int., 162, pp: 633–640.

Bozkurt, E., and M. Satir, 2000, The Southern Menderes Massive (Western Turkey): Geochronology and Exhumation History, Geol. Journal, 35, pp: 285–296.

Bozkurt, E. and R. Oberhaensli, 2001, Menderes Massive (Western Turkey): Structural, Metamorphic and Magmatic Evolution: A Synthesis, Int J Earth Sci, 89, pp: 679–708.

Candan, O., Ö. Dora, R. Oberhänsli, M. Çetinkaplan, J. Partzsch, F. Warkus, and S. Dürr, 2001, Pan-African High-Pressure Metamorphism in the Precambrian Basement of the Menderes Massive, Western Anatolia, Turkey, Int. Journal of Earth Sciences, 89, pp: 793–811.

Çakmakoğlu, A., 2007, Pre-Neogene Tectono-Stratigraphy of Dilek Peninsula and the Area Surrounding Söke and Selçuk, Bulletin of Mineral Research and Exploration of Turkey (MTA), 135, pp: 1–17.

Dolmaz, M. N., Z.M. Hisarli, T. Ustaömer, and N. Orbay, 2005, Curie Point Depths Based on Spectrum Analysis of the Aeromagnetic Data, West Anatolian Extensional Province, Turkey, Pure and Appl. Geop., 162, pp: 571–590.

Geosystem, 2009, Data Modelling and Interpretation of Magnetotelluric Surveys Küçük and Büyük Menderes Graben, Turkey," BM Engineering and Construction Inc. Internal Report, 109 Pages.

Gessner, K., U. Ring, C. Passchier, and T. Güngör, 2001, How to Resist Subduction: Evidence for Large-Scale Out-of-Sequence Thrusting During Eocene Collision in Western Turkey, J. of Geo. Soc. of London, 158, pp: 769–784.

Ilkisik, O.M., 1995, Regional Heat Flow in Western Anatolia Using Silica Temperature Estimates From Thermal Springs, Tectonophysics, 244, pp: 175–184.

Koçyiğit, A., 2009, Active Tectonics of Söke-Argavlı and Gümüşköy Area, BM Engineering and Construction Inc., BM Engineering and Construction Inc., Internal report 26 pages.

KOERI, Boğaziçi University Kandilli Observatory and Earthquake Research Institute (2010), http://www.koeri.boun.edu.tr (accessed September, 2010).

Kuyumcu, Ö. Ç., U.Z. Destegül, and A.Ü. Akman, 2010, Exploration and Discovery of the Gümüşköy Geothermal Reservoir in Aydın, Turkey, GRC Transactions, v. 34., pp: 575–580

MTA, Turkish Geothermal Resources Inventory, MTA, Ankara (2005), 849 pages.

Okay, A. I., 2001, Stratigraphic and Metamorphic Inversions in the Central Menderes Massive; a New Structural Model, Int J Earth Sci, 89, pp: 709–727.

Petrel*, 2010, Schlumberger Information Solution, Petrel Software Online Help

http://www.slb.com/services/software/geo/petrel.aspx

Pfister, M., W. Balderer, E. Greber, H.G. Kahle, D.M. Rossa, S. Mueller, L. Rybach, C. Shinder, S. Sellani, and C. Straub, 1997, Synthesis of the Marmara Poly-Project". In: Schindler, C., Pfister, M. (eds.), "Active Tectonics of Northwestern Anatolia, The Marmara Poly-Project, VDF, Hoschschulverlag AG An Der EFH, Zürich, pp:539–565.

Ring, U., K. Gessner, T. Güngör, T. and. C.W. Passchier, 1999, The Menderes Massive of Western Turkey and the Cycladic Massive in the Aegean–Do They Really Correlate?, Journal of the Geological Society of London, 156, pp: 3–6.

Ring U., C. Johnson, R. Hetzel, K. Gessner, 2003, Tectonic Denudation of a Late Cretaceous–Tertiary Collusional Belt: Regionally Symmetric Cooling Patterns and Their Relation to Extensional Faults in the Anatolide Belt of Western Turkey, Geol. Mag., No. 140 (4), pp: 421–441.

Rimmelé, G., T. Parra, B. Goffé, R. Oberhänsli, L. Jolivet, and O. Candan, 2004, Exhumation Paths of High-Pressure-Low-Temperature Metamorphic Rocks from the Lycian Nappes and the Menderes Massive (SW Turkey): a Multi-Equilibrium Approach," Journal of Petrology, pp: 1–29.

Sengör, A.M.C., M. Satir, and R. Akkök, 1984, "Timing of the Tectonic Events in the Menderes Massive, Western Turkey: Implications for Tectonic Evolution and Evidence for Pan-African Basement in Turkey, Tectonics, no. 3, pp: 693–707.

Tüysüz, O., Ş.C. Genç, 2010, Geology of the Söke-Ortaklar-Selçuk Area, BM Engineering and Construction Inc., Internal Report 39 pages.

Yıldırım, N., 2009, Büyük Menderes Ortaklar-Gümüşköy-Söke Geothermal Project–Hydrogeochemical and Physıcochemical Pre-Feasibility Study Report, BM Engineering and Construction Inc., Internal Report 44 pages.